HHS Public Access

Author manuscript

Lasers Surg Med. Author manuscript; available in PMC 2020 April 01.

Published in final edited form as:

Lasers Surg Med. 2019 April ; 51(4): 345–351. doi:10.1002/lsm.23019.

Development and Evaluation of a Low-Cost, Portable, LED-Based Device for PDT Treatment of Early-Stage Oral Cancer in Resource-Limited Settings

Hui Liu[1], **Liam Daly**[2], **Grant Rudd**[2], **Amjad P. Khan**[3], **Srivalleesha Mallidi**[3], **Yiran Liu**[1], **Filip Cuckov**[2], **Tayyaba Hasan**[3], **Jonathan P. Celli**[1]

[1]Department of Physics, University of Massachusetts, Boston, Massachusetts 02125

[2]Department of Engineering, University of Massachusetts, Boston, Massachusetts 02125

[3]Wellman Center for Photomedicine, Massachusetts General Hospital, Boston, Massachusetts 02114

Abstract

Background: Photodynamic therapy (PDT) using δ-aminolevulinic acid (ALA) photosensitization has shown promise in clinical studies for the treatment of early-stage oral malignancies with fewer potential side effects than traditional therapies. Light delivery to oral lesions can also carried out with limited medical infrastructure suggesting the potential for implementation of PDT in global health settings.

Objectives: We sought to develop a cost-effective, battery-powered, fiber-coupled PDT system suitable for intraoral light delivery enabled by smartphone interface and embedded electronics for ease of operation.

Methods: Device performance was assessed in measurements of optical power output, spectral stability, and preclinical assessment of PDT response in ALA-photosensitized squamous carcinoma cell cultures and murine subcutaneous tumor xenografts.

Results: The system achieves target optoelectronic performance with a stable battery-powered output of approximately 180 mW from the fiber tip within the desired spectral window for PpIX activation. The device has a compact configuration, user friendly operation and flexible light delivery for the oral cavity. In cell culture, we show that the overall dose-response is consistent with established light sources and complete cell death of ALA photosensitized cells can be achieved in the irradiated zone. In vivo PDT response (reduction in tumor volume) is comparable with a commercial 635 nm laser.

Conclusions: We developed a low-cost, LED-based, fiber-coupled PDT light delivery source that has stable output on battery power and suitable form factor for deployment in rural and/or resource-limited settings.

*Correspondence to: Jonathan P. Celli, Department of Physics, University of Massachusetts, 100 Morrisey Blvd, Boston, Massachusetts, 02125. jonathan.celli@umb.edu.

Conflict of Interest Disclosures: All authors have completed and submitted the ICMJE Form for Disclosure of Potential Conflicts of Interest and none were reported.

Keywords

photodynamic therapy (PDT); Oral Cancer; light emitting diode (LED); global health; aminolevulinic acid (ALA); protoporphhyrin IX (PpIX)

INTRODUCTION

The high incidence and dismal outcomes for oral cancer in south Asia have been described as a global health crisis [1,2]. In India, due to the widespread popularity of chewing paan, gutka, or other tobacco mixtures there is an exceptionally high incidence of oral cancers, which account for over 30% of cancers reported and are the leading cause of cancer death among Indian men [2]. Standard treatments for oral cancers include surgery, chemo, and radiation therapy. Treatment may be curative if disease is diagnosed sufficiently early but even then side effects and disfigurement from treatment may compromise a patient's ability to chew, swallow, and speak [1]. Moreover, access to suitable treatment in rural settings is often limited due to a lack of local medical facilities able to support complex surgical procedures and/or radiotherapy [3]. Motivated by all these factors there is need to explore treatment options for oral cancer that are effective and which can be implemented in sites with limited medical infrastructure.

Photodynamic therapy (PDT) is a light-based treatment modality in which a photosensitizer or precursor is delivered to target tissue prior to therapeutic activation using light of the appropriate wavelength and irradiance [4,5]. Clinical studies of PDT for the treatment of oral cancer have indicated that it is a viable approach, achieving complete epithelial necrosis and with excellent healing of the mucosa [6–11]. Notwithstanding a lack of large-scale controlled trials, thousands of individual head and neck cancer patients with premalignant, malignant, or advanced cancer, including tumors that are refractory to chemo and radiotherapies have been successfully treated with PDT worldwide [12]. Also, for applications where light delivery can be achieved at the tissue surface (without need for intraoperative or interstitial light delivery), PDT procedures can be conducted without requirements for extensive medical infrastructure. Activation of the photosensitizer can be accomplished with relatively low cost LED light sources can be used as an alternative to traditional medical lasers [6,11,13–17] and which can be engineered to operate in battery power in settings with unreliable electrical power supply. Furthermore, imaging of photosensitizer fluorescence can be leveraged for treatment guidance and monitoring can be carried out using a consumer smartphone, also allowing potential for telemedicine integration [16,17]. If accompanied by development of simple to use light sources with predictable dosimetry these features point to the potential of PDT as an effective oral cancer treatment modality for global health settings.

To address the technology adaptation needs noted above we sought to develop a compact and portable, battery-operated, fiber optic coupled LED-based light source suitable for treatment of small, T1 oral lesions (≤ 2 cm in diameter). To treat disease of this size with total fluence at the tissue surface for 100 J/cm^2 delivered within a reasonable time frame (less than 1 hour including fractionation breaks) a fluence rate at tissue surface of at least 30

mW/cm^2 is required. For portability in rural sites the light source should be small enough to transport on a bicycle. Stable operation on battery power is highly desirable for use in resource-limited settings with inadequate electrical infrastructure. The whole system has four major parts: the LED fiber optic device, a digitally controlled LED driver, a touchscreen user interface, and a smart-phone App which enables Bluetooth operation. In this report we describe the development, hardware testing, and preclinical validation of a 635 nm LED-based light source for ALA PDT which meets the above requirements.

MATERIALS AND METHODS

Optoelectronic Design

For flexible intra-oral light delivery, we used a 1 mm multi-mode optical fiber (Thorlabs M59L01) coupled to a high intensity LED with integrated SMA fiber mount (Innovations in Optics, 1700A-100 LED). Optical power and spectral measurements were made with a photodetector (Thorlabs S121C) with power meter console (Thorlabs PM100) and a spectrometer (Ocean Optics USB2000), respectively. We chose an aluminum enclosure for better heat conduction and made a customized battery compartment to accommodate a high capacity rechargeable lithium-polymer battery. The LED panels adhere to a passive heat sink with a fan attached to the rear panel of the instrument. To prevent drop in output power while running on battery source we designed the LED driver to regulate a constant-drive current to power the LED. The high conversion efficiency, low heat dissipation, and small size of the driver circuit make it highly suitable for use in a portable, battery-powered device. For practical consideration, we included an aiming mode to facilitate physicians with initial positioning. It runs at low current (around 250 mA) to avoid high PpIX breakdown. A single LM317 voltage regulator is used to regulate this minimal current in a constant-current mode, which is enabled digitally using a relay. We also used additional voltage regulators to provide power to the microcontroller and its peripherals, the cooling fans, and the touch-screen display. We tested the optical power stability of the fiber delivery end within 30 min operation window using a lithium-polymer (Lipo) battery as the power source (Gens ace 7.4V 6000mAh 70C LiPo Battery Pack 2S).

Design of PDT Device and Embedded Systems for Device Control

The battery-operated PDT device is shown in Figure 1. A compact AVR microcontroller platform (Teensy 3.2 microcontroller) digitally controls the LED driver. The microcontroller also operates 3.5inch resistive touchscreen, providing an on-device user interface, and uses Bluetooth for smartphone interface and control. At the user end, both the touch-screen interface and the smart-phone program can control the illumination of the LED and operate a treatment timer. The touch screen operation also shows the remaining percentage of the battery charge on the top right. Figure 1b shows the simplified flow chart of the embedded system software design, which follows an event-driven design pattern. The data is collected and filtered by a timer-based interrupt routine from a resistive touchscreen and is parsed into event messages which are written to an event buffer. The main thread reads the battery voltage, updates the timer, handles incoming Bluetooth data, changes the TFT display *via* an SPI bus, and then responds to any messages appearing in the event queue. In the interrupt thread, event messages are generated when a touch action is initiated or released or when a

sustained touch moves from the area of one user interface element, such as a button, to another such area. The prototype device is shown in Figure 1c. The dimensions of the device are 33 × 26 ×12 cm and total cost is about $700 at the time of this report.

Cell Culture and *In Vitro* Experiments

A431 squamous carcinoma cells were obtained from American Type Culture Collection (ATCC, Rockville, MD) and grown in DMEM (HyClone, Logan, Utah) supplemented with 10% FBS (HyClone), 100 IU/ml penicillin (Life Technologies, Carlsbad, CA), and 100 μg/ml streptomycin (Life Technologies). Cell cultures were maintained at 378C in a humid atmosphere of 95% air and 5% CO_2 and harvested for treatment assessment studies either in multiwell plates (for *in vitro* studies) or for murine tumor implantation as described below. For *in vitro* dose response experiments 96 well plates were used with three replicate wells for each treatment condition and control group. For cell kill area measurements cultures were plated in 35 mm dishes with each treatment condition in triplicate. In both cases cultures were photosensitized using 2.0 mM 5-ALA (Sigma–Aldrich) in media for 4 hours prior to light activation. Light was delivered at 30 mW/cm^2 either continuously or fractionated as indicated by mounting the fiber optic vertically underneath the cell culture vessel as in previous *in vitro* PDT experiments [14,16].

Image-Based Treatment Assessment

The treatments were evaluated by imaging after 24 hours, which allows sufficient time for apoptosis. Cell cultures were labeled with fluorescent vital dyes Calcein AM and Ethidium Bromide (Life Technologies). We chose the central region of the treated area, and 5× mosaic images of cell culture were obtained from the irradiated region of each well. The imaging was taken with a Zeiss AxioObserver microscope (Carl Zeiss). The microscope is equipped with a cooled, high-resolution monochromatic 14-bit digital camera (AxioCam, Carl Zeiss). Images were segmented using MATLAB routines (Mathworks, Natick, MA) to quantify the size of the cell killing region in fluorescent images using an adaptation of previously reported methods [18].

Animal Model and *In Vivo* PDT

All animal studies were approved by the Subcommittee on Research Animal Care at the Massachusetts General Hospital and conformed to the guidelines established by the NIH. Briefly, four-to-six- week-old female immunos-compromised Swiss nude mice weighing between 20 to 25 g were obtained from Cox Breeding Laboratories, Cambridge, Massachusetts. A431 human epidermoid carcinoma cells of low passage number (<20) in monolayer were collected and resuspended in phosphate buffered saline (PBS), and 50 ml containing 2.5 ×10^6 cells mixed with 50 μl Matrigel were injected subcutaneously into the right scapular region. The tumors were allowed to grow until they reached about 20–60 mm^3 in volume (10 days after implantation), at which point animals were assigned to PDT using the LED light source (LED-PDT) or a commercial 635 nm laser source (Model 7401; Intense, North Brunswick, NJ). Three mice per group were assigned to control (no treatment) group, 100 J/cm^2 delivered by LED device and 100 J/cm^2 delivered *via* commercial laser. The tumor-bearing mice were administered ALA intravenously at 200 mg/kg. After 2 hours transcutaneous irradiation of the tumor delivered by fiber through the

skin at a fluence rate of 30 mW/cm^2 with the total fluence of 100 J/cm^2 was performed using either the LED or the laser light. The tumor volume was estimated at each time point listed *via* ultrasound using a VisualSonics high frequency ultrasound imaging system fitted with a MS550S probe. 3D scans were performed to obtain tumor length l, breadth b, and height h and volumes calculated as $V = \frac{\pi}{2} lbh$. To correct for variation in initial tumor volume the measured volume at each time point was normalized to the initial volume for that tumor, V_0. PpIX fluorescence was measured using a whole animal *in vivo* imaging system (IVIS, Perkin Elmer) on anesthetized mice before and after PDT light delivery. Significance of comparison between groups was evaluated using a two-tailed Student's t-test.

RESULTS

LED Device Performance: Measurements of Optical Power Stability and Spectral Properties

We first characterized optical output power stability (Fig. 2a), and spectral properties (Fig. 2b) of the LED source. These measurement were performed at various driving current and in each case established stability of output while operating on battery power, with less than 4% power fluctuation from beginning to end of monitoring (30 minutes). This is a significant improvement over our previously reported device which exhibited slow but continuous optical power drop during battery operation [16,17]. The optical power at the fiber delivery end increases with the driving current with diminishing returns on electrical input power approaching 10A (Fig. 2b). While the spectral shape remains the same, the central wavelength of the emission light shifts from 634.5 nm at 4A to 644.5 nm at 10A (Fig. 2c and d). The shift to longer wavelength at higher currents (and operating temperature) is expected for LED sources but prompts a concern that the benefit of gain in power may not be useful if the emission spectrum no longer has sufficient overlap with the target absorption band (in this case for PpIX).

To optimize the selection of device operating current the spectral overlap area, A, between the desired PpIX absorption band (around 635 nm), and the current-dependent LED emission spectra scaled by total optical power P at each operating current tested (Fig. 3). The effective absorption is given by $A_{eff} = A \times P$. As shown in Figure 3b, the gain in total power at higher currents is offset by decreasing spectral overlap with PpIX absorption band around 635 nm. In other words, more power is output at higher currents but not at optimal wavelengths. Motivated by this tradeoff we selected an operating current of 7A, which roughly maximizes spectral efficiency and avoids unnecessary heating and wasted battery drain.

Assessment of PDT Response Using the Battery-Powered LED Device

In ALA-photosensitized A431 cell cultures in multiwell plates treated the LED device we observe increased cell killing with increased total light dose deliveted (Fig. 4a). Since it is also well known that fractionated irradiation can enhance PDT efficacy [8,19,20], we examined a simple fractionation regimen with total dose divided into three equal fractions divided by 1-minute breaks. Continuous and fractionated delivery is compared for 40 and 60

J/cm^2, both at 80 mW/cm^2 fluence rate, showing modest benefit of fractionation in each case (Fig. 4b)

Assessment of Effective Zone of Cell Killing for Varying Beam Spot Size

We tested the effective cell killing areas for anticipated sizes of small (early stage) oral lesions on the order of 1–2 cm in diameter, by performing treatments on confluent monolayers in 35 mm dishes using three independent measurements for each beam diameter. Interestingly, Figure 5 shows that the effective killing area measured by vital dye staining after treatment is consistently slightly larger than that of the illuminated spot size, which is likely the result of refraction or a modest bystander effect to cells just outside the spot radius [21,22]. The image thresholding to identify the effective zone of cell death was performed using raw image data though display image in Figure 5 was adjusted using the HiLo lookup table for clarity.

Validation of LED Device Performance *In Vivo*

We compared response to ALA PDT in murine xenografts using the LED source and a commercial laser source. In both cases treatment parameters were kept consistent with a fluence rate of 30 mW/cm^2 at tissue surface, and a fluence of 100 J/cm^2. Endpoints assessed were tumor volumes measured by ultrasound and relative PpIX fluoresnece photobleaching. Both light sources provide an effective PDT response with clear reduction in tumor volume relative to untreated mice (Fig. 6a). A modest enhancement is observed in laser treated mice relative to the LED but the difference is not statistically significant ($P > 0.05$, two tailed *t*-test). It is likely that the effective dose deposited by the laser is slightly higher due to the broader spectral width of the LED as discussed below. Extent of PpIX photobleaching is approximately the same for both light sources.

DISCUSSION

In this study we describe the development and validation of a fiber-coupled LED light source for PDT that is specifically designed to be battery-operated, cost effective and portable. It is worth noting that the decision to use an LED rather than a diode laser is motivated by cost and relative simplicity of driving electronics though does come with tradeoffs in spectral properties and beam divergence. With an optical fiber coupling efficiency of only about 10% for the LED used here there is major power loss even using a relatively thick (1 mm) fiber. This is nevertheless deemed necessary by the gain in flexibility from using a fiber, especially for the envisaged application of the present device in which the fiber tip can be coupled to appropriate size and shape applicator for intraoral delivery. Since LEDs have broader spectral width in comparison to a laser it is expected that greater efficiency of photoactivation per unit optical power delivered will be achieved with a laser, assuming that its emission wavelength is well matched to the photosensitizer absorption peak. On the other hand, if the peak source wavelength is not optimally matched to a narrow target absorption band then the spread of optical power over a broader spectral window that an LED provides may be advantageous.

Another design consideration of the device introduced here is the use of embedded systems for feedback and control. By including embedded control the intent is to enable future interface with a potentially wide range of other interfacing devices, allowing for example adaptive changes to dose rate and other treatment parameters in response to real time monitoring from imaging or tissue oxygenation measurements.

CONCLUSION

We have developed and demonstrated the efficacy of a portable LED-based, battery-operated PDT light source with user friendly interface and flexible light delivery. Although our system was designed to meet specific engineering criteria for intraoral light delivery in resource-limited settings, those same characteristics could also be beneficial in a traditional clinical setting or even as a reliable and cost-effective research tool for laboratory-based preclinical PDT studies.

ACKNOWLEDGMENTS

We gratefully acknowledge funding from the National Institutes of Health, UH2 CA1889901 (to TH and JPC), UH3 CA189901 (to Tayyaba Hasan and Jonathan P. Celli and S10 0D01232601 (to TH). We are also grateful for productive conversations with Dr. Stephen Bown and Dr. Colin Hopper of the National Medical Laser Centre in the U.K., Dr. Maria Troulis and Dr. Meredith August of the Dept of Oral and Maxillofacial Surgery at Massachusetts General Hosptial, and Dr. Shahid Siddiqui, Dr. Bilal Hussain, and Dr. Abrar Hasan at JN Medical College, Aligarh Muslima University, India

Contract grant sponsor: NIH; Contract grant numbers: S10 0D01232601, UH2 CA1889901, UH3 CA1889901.

REFERENCES

1. Casiglia J, Woo SB. A comprehensive review of oral cancer. Gen Dent 2001;49(1):72–82. [PubMed: 12004680]
2. Rodu B, Jansson C. Smokeless tobacco and oral cancer: a review of the risks and determinants. Crit Rev Oral Biol Med 2004;15(5):252–263. [PubMed: 15470264]
3. Coelho KR. Challenges of the oral cancer burden in India. J Cancer Epidemiol 2012; 2012: 701932. [PubMed: 23093961]
4. Celli JP, Spring BQ, Rizvi I, et al. Imaging and photodynamic therapy: mechanisms, monitoring, and optimization. Chem Rev 2010;110(5):2795–2838. [PubMed: 20353192]
5. Felsher DW. Photodynamic therapy for cancer. Nat Rev Cancer 2003;3(5):375–380. [PubMed: 12724735]
6. Chen HM, Yu CH, Lin HP, Cheng SJ, Chiang CP. 5- Aminolevulinic acid-mediated photodynamic therapy for oral cancers and precancers. J Dent Sci 2012;7(4):307–315.
7. Fan KF, Hopper C, Speight PM, Buonaccorsi G, MacRobert AJ, Bown SG. Photodynamic therapy using 5-aminolevulinic acid for premalignant and malignant lesions of the oral cavity. Cancer 1996;78(7):1374–1383. [PubMed: 8839541]
8. Gallagher-Colombo SM, Quon H, Malloy KM, et al. Measuring the physiologic properties of oral lesions receiving fractionated photodynamic therapy. Photochem Photobiol 2015;91(5): 1210–1218. [PubMed: 26037487]
9. Grant WE, Hopper C, MacRobert AJ, Speight PM, Bown SG. Photodynamic therapy of oral cancer: photosensitisation with systemic aminolaevulinic acid. Lancet 1993;342(8864): 147–148. [PubMed: 7687318]
10. Kubler A, Haase T, Rheinwald M, Barth T, Muhling J. Treatment of oral leukoplakia by topical application of 5- aminolevulinic acid. Int J Oral Maxillofac Surg 1998;27(6): 466–469. [PubMed: 9869290]

11. Tsai JC, Chiang CP, Chen HM, et al. Photodynamic Therapy of oral dysplasia with topical 5-aminolevulinic acid and light- emitting diode array. Lasers Surg Med 2004;34(1):18–24. [PubMed: 14755421]
12. Pei-Jen L, Linda J, Colin H. Clinical outcomes of photodynamic therapy for head-and-neck cancer. Technol Cancer Res Treat 2003;2(4):311–317. [PubMed: 12892513]
13. Chen H-M, Yu C-H, Tu P-C, Yeh C-Y, Tsai T, Chiang C-P. Successful treatment of oral verrucous hyperplasia and oral leukoplakia with topical 5-aminolevulinic acid-mediated photodynamic therapy. Lasers Surg Med 2005;37(2):114–122. [PubMed: 16037967]
14. Liu H, Rudd G, Daly L, et al. Development of low-cost devices for image-guided photodynamic therapy treatment of oral cancer in global health settings. In: SPIE BiOS: 2016: SPIE; 2016: 6.
15. Yu CH, Lin HP, Chen HM, Yang H, Wang YP, Chiang CP. Comparison of clinical outcomes of oral erythroleukoplakia treated with photodynamic therapy using either light- emitting diode or laser light. Lasers Surg Med 2009;41(9): 628–633. [PubMed: 19816916]
16. Hempstead J, Jones DP, Ziouche A, et al. Low-cost photodynamic therapy devices for global health settings: characterization of battery-powered LED performance and smartphone imaging in 3D tumor models. Sci Rep 2015; 5: 10093. [PubMed: 25965295]
17. Mallidi S, Mai Z, Rizvi I, et al. In vivo evaluation of battery-operated light-emitting diode-based photodynamic therapy efficacy using tumor volume and biomarker expression as endpoints. J Biomed Opt 2015;20 (4): 048003. [PubMed: 25909707]
18. Celli JP, Rizvi I, Blanden AR, et al. An imaging-based platform for high-content, quantitative evaluation of therapeutic response in 3D tumour models. Sci Rep 2014; 4:3751. [PubMed: 24435043]
19. Müller S, Walt H, Dobler-Girdziunaite D, Fiedler D, Haller U. Enhanced photodynamic effects using fractionated laser light. J Photochem Photobiol B 1998;42(1):67–70. [PubMed: 9491597]
20. Pogue BW, Hasan T. A theoretical study of light fractionation and dose-rate effects in photodynamic therapy. Radiat Res 1997;147(5):551–559. [PubMed: 9146700]
21. Dahle J, Bagdonas S, Kaalhus O, Olsen G, Steen HB, Moan J. The bystander effect in photodynamic inactivation of cells. Biochim Biophys Acta 2000;1475(3):273–280. [PubMed: 10913826]
22. Poyer F, Thomas CD, Garcia G, et al. PDT induced bystander effect on human xenografted colorectal tumors as evidenced by sodium MRI. Photodiagnosis Photodyn Ther 9(4):303–309. [PubMed: 23200010]

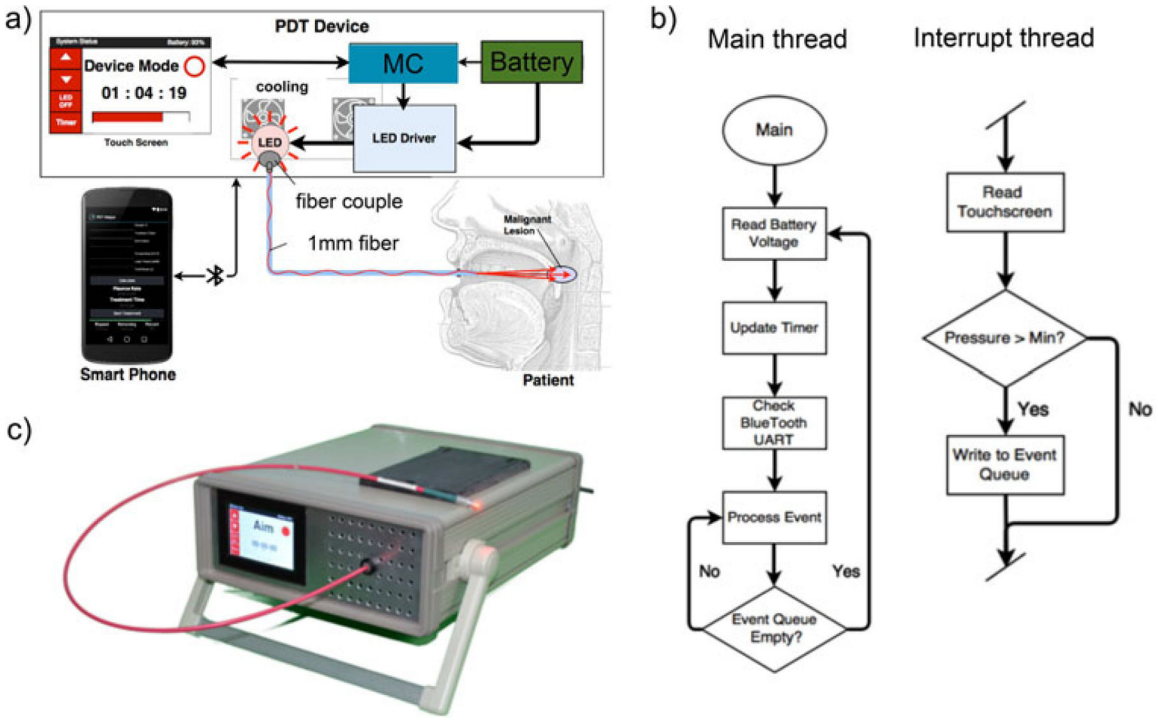

Fig. 1.

(**a**) Schematic of smartphone-controlled PDT device (MC, micro-controller). (**b**) Simplified flowchart of embedded systems for device control (**c**) Photo of a prototype device.

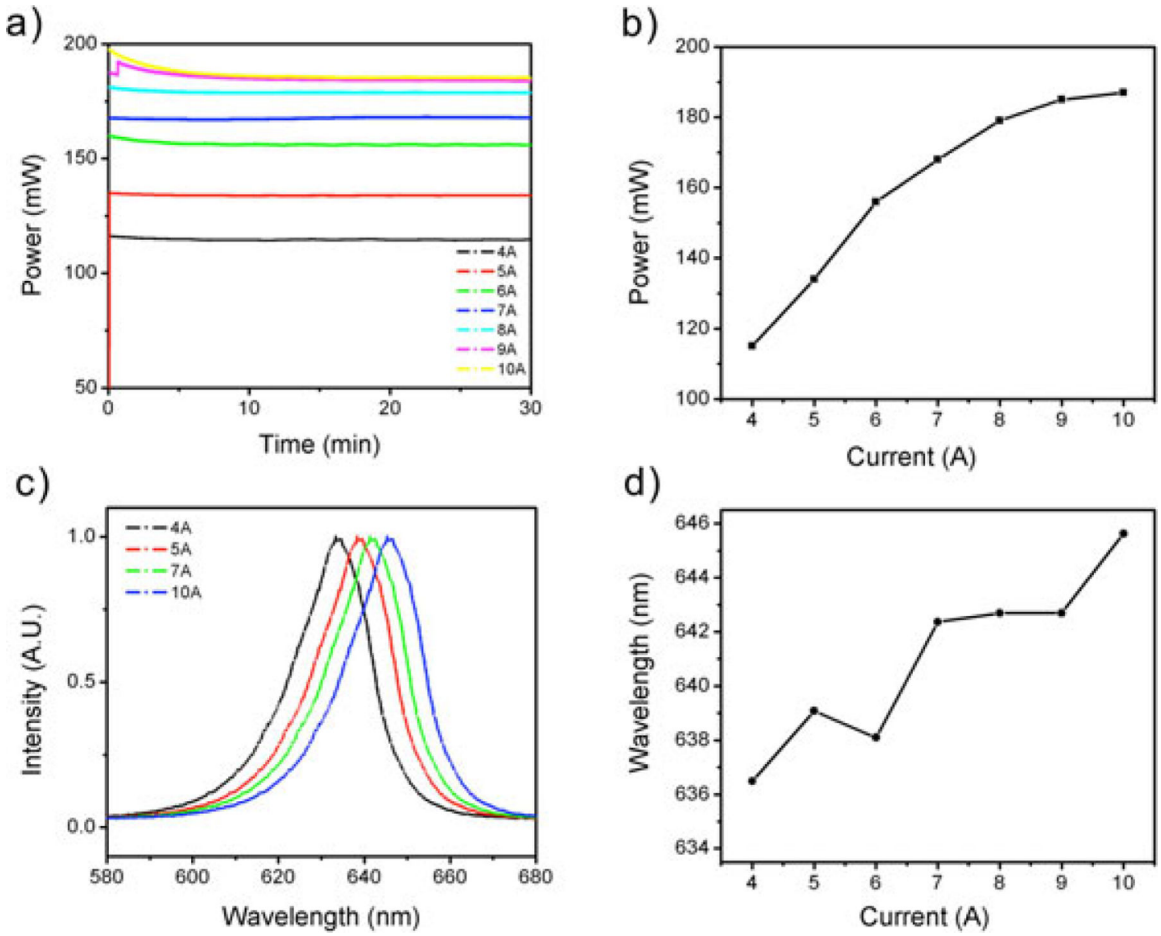

Fig. 2.

Optical power output and spectral stability. The battery-powered device achieves excellent optical power stability at any given operating current but (as expected for an LED device), exhibits spectral shifts to increased l at higher current (and power). (**a**) Measured LED output power (after fiber) is stable up to a driving current of 8A. (**b**) Total optical power output increases with driving current as expected, but with diminishing returns at higher current. (**c,d**) Spectral data showing LED peak emission wavelength at different operating current after a 1-hour continuous operation (**c**).

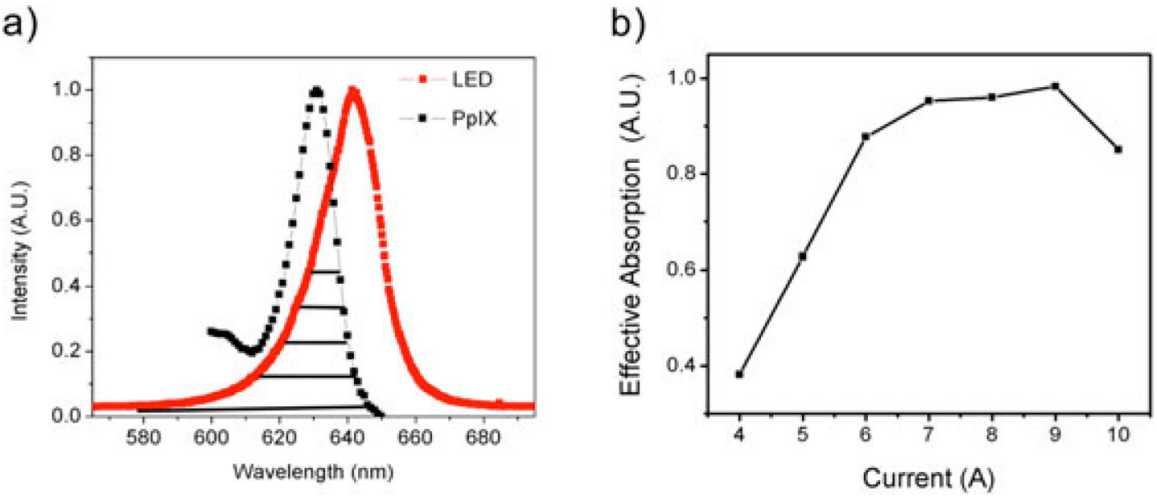

Fig. 3.

Effective absorption optimization with consideration of the absorption spectrum of PpIX and power increase. As current is increased, the optical power is also increased, but effective PpIX activation is also impacted by spectral shifts in LED emission with increasing current. (**a**) Overlap in PpIX absorption spectrum and LED emission spectrum at 7A operating current. The overlapped area under PpIX and each LED spectral is the effective absorption for the specific LED spectrum. (**b**) Calculated effective PpIX absorption over a range of LED driving currents shows saturation at high currents and suggests there is no benefit in driving the LED at higher than approximately 7A.

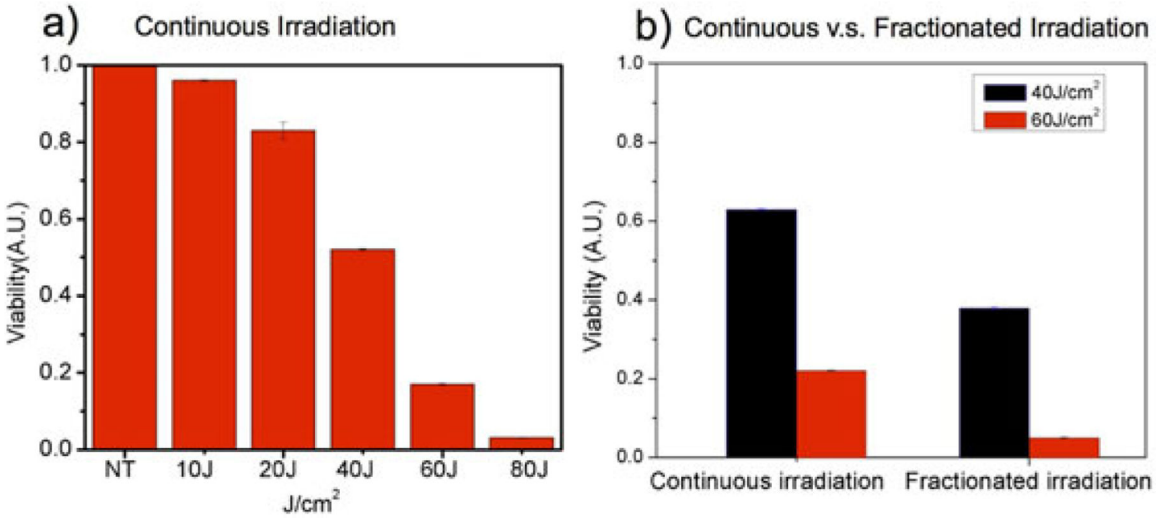

Fig. 4.

ALA PDT response in squamous carcinoma cells using battery powered LED source. (**a**) Dose response with continuous irradiation (each condition averaged over three replicates and normalized to no treatment, NT). (**b**) Comparison of fractionated and continuous irradiation at 40 J/cm^2 and 60 J/cm^2. Error bars represent standard error.

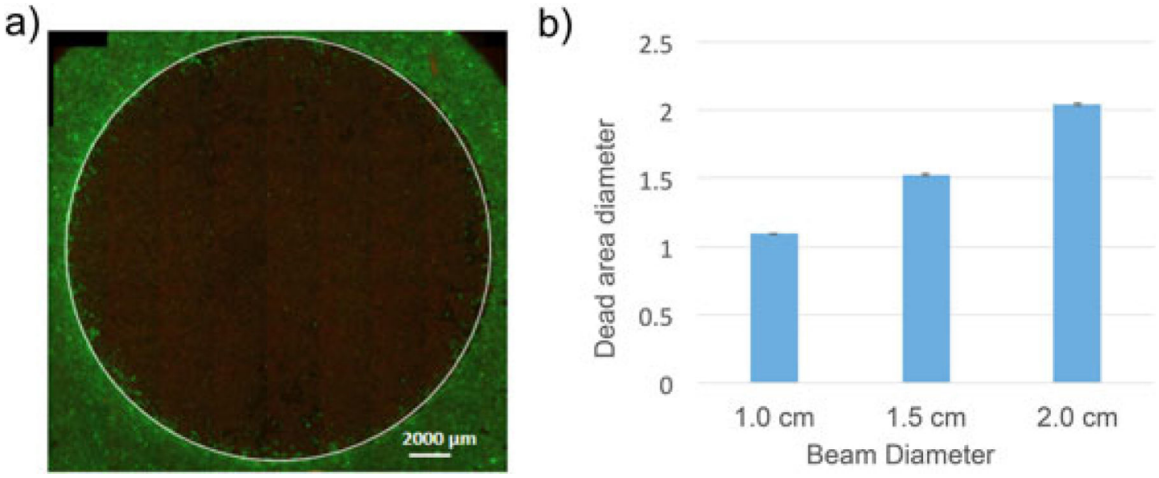

Fig. 5.

(**a**) Representative fluorescence image showing effective PDT cell killing area (indicated by the white circle) in A431 cells stained with vital dyes (live cells green, dead cells red). PDT treatments were carried out on ALA photosensitized cells (4 hour ALA incubation). A total dose of 100 J/cm^2 was delivered for three beam spot sizes at the same total optical power but compensating for decreased irradiance from beam expansion with increased irradiation duration in the same proportion. (**b**) The mean killing diameter from image segmentation is consistent with spot size with 1, 1.5, and 2 cm beams achieving 1.09 cm (± 0.3%), 1.53 cm (± 1%), and 2.04 cm (±0.9%), respectively. Error bars show standard error.

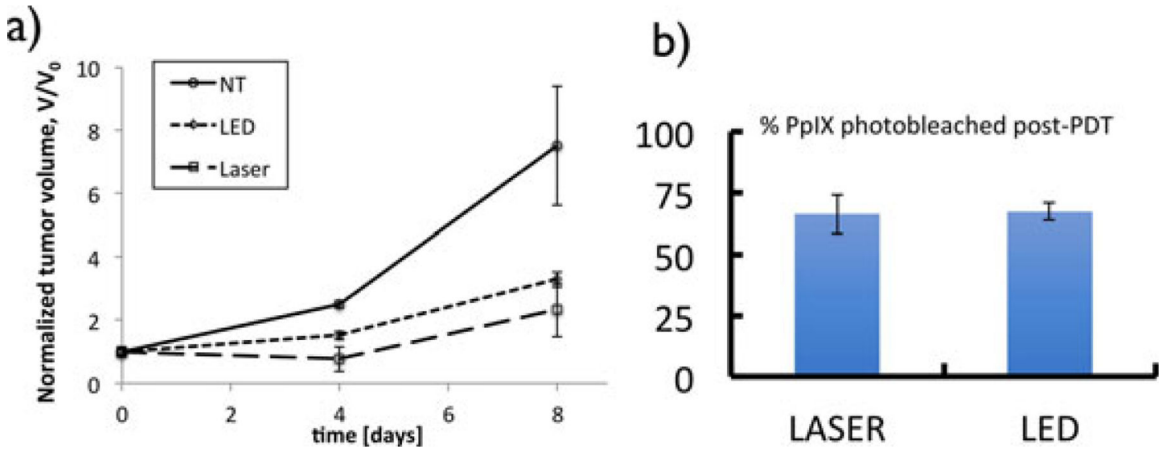

Fig. 6.

Comparison of ALA PDT response *in vivo* using LED device and a laser source. (**a**) Comparison of volume 10 days after PDT treatment with each light source. Both light sources produce effective tumor response. The difference in response for LED and laser groups is not statistically significant ($P > 0.05$) at either time point. (**b**) The extent of PpIX photobleaching (ratio of post-PDT to pre-PDT fluorescence) is approximately the same for both light sources.